

Denver, Colorado  
**NOISE-CON 2013**  
2013 August 26-28

## Noise Source Identification on a Stageloader System

Hugo E. Camargo  
David S. Yantek  
Robert Randolph  
National Institute for Occupational Safety and Health  
Office of Mine Safety and Health Research  
626 Cochrans Mill Road  
Pittsburgh, PA 15236  
[HCamargo@cdc.gov](mailto:HCamargo@cdc.gov)

Kyle Schwartz  
Patricio Ravetta  
Ricardo Burdisso  
AVEC, Inc.  
3154 State Street, Suite 2230  
Blacksburg, VA 24060

*The findings and conclusions in this report are those of the author(s) and do not necessarily represent the views of the National Institute for Occupational Safety and Health (NIOSH). Mention of any company name, product, or software does not constitute endorsement by NIOSH.*

### ABSTRACT

Longwall mines provide approximately half of the U.S. national underground coal production. However, longwall systems often expose workers to hazardous noise. The National Institute for Occupational Safety and Health (NIOSH) measured sound levels well over 100 dB(A) at worker locations. Furthermore, 48% of noise samples collected at shearer longwalls by the Mine Safety and Health Administration exceeded that agency's permissible exposure level.

NIOSH is currently conducting research to develop noise controls for longwall systems. The two most significant sound-radiating components of a longwall system are the shearer and the stageloader. This paper presents a noise source identification effort for a stageloader as the first step to developing noise controls. Due to the lack of instrumentation approved for use in underground coal mines, the present study was conducted on a new stageloader in a manufacturer's building. A 63-microphone array was used for the test and data were processed using conventional beamforming. Results showed that the frequency content of the most prominent sources was towards the lower end of the spectrum (<1,900 Hz). The location of the most dominant sources was in the region of the electric motor and where the conveyor chain either radiated noise itself or directly excited other component such as the side wall plates on the output side.

### 1. INTRODUCTION

Longwall mining systems are used where geological factors permit because of their efficiency in extracting coal. Longwall mines are responsible for providing approximately half of the total U.S. underground coal production. However, longwall systems often expose workers to hazardous noise. The National Institute for Occupational Safety and Health (NIOSH) has measured sound levels well over 100 dB(A) at worker locations in longwall mines<sup>1</sup>. Furthermore, analysis of noise samples collected at shearer longwalls by the Mine Safety and Health Administration (MSHA) indicated that 48% of the samples exceeded that agency's permissible exposure level<sup>2</sup>. Consequently, NIOSH is conducting research to develop engineering noise controls for longwall mining systems.

Noise surveys conducted in underground longwall mines have found that most of the sound from longwall systems was radiated from two system components—the shearer and the stageloader<sup>3</sup>. The current study investigated noise from the stageloader, which is used to crush the coal extracted from the face and load it on a conveyor belt to be transported out of the mine. A noise source identification procedure was conducted on a new stageloader machine using phased array technology. Noise source identification is the first step in the noise control development process. The main objective of the phased array measurements was to identify the noise sources on a stageloader and assess their frequency content.

## 2. DESCRIPTION OF A LONGWALL SYSTEM

Longwall systems are sets of machines that work in full synchrony to extract ore from underground mines. Although there are two basic types of longwall systems—shearers and plows—in the United States approximately 98% of longwall mines use shearers<sup>4</sup>. For this reason, the work presented in this paper focuses on longwall shearer systems. These systems are mainly used in coal and in a few iron mines throughout the United States; therefore, the terms “coal” and “ore” will be used interchangeably throughout the paper.

As shown in Figure 1, a longwall system is comprised of the following components: a shearer that traverses back and forth along the face, ripping coal; an armored face conveyor (AFC) that runs along the face and transports the ripped coal to the stageloader; powered self-advancing longwall shields that provide temporary roof support for the shearer and the AFC; and the stageloader which, after crushing the coal, loads it onto a belt conveyor to be taken out of the mine. The shearer measures from 8 to 12 meters in length, and by virtue of its ranging arms can perform cuts of 2 to 6 meters in height. Each shield measures from 1.5 to 2 meters in width, and therefore on a typical 400-meter-long face there are over 200 shields providing the temporary roof support. Since the AFC runs along the face, typical AFCs can measure 400 meters in length.

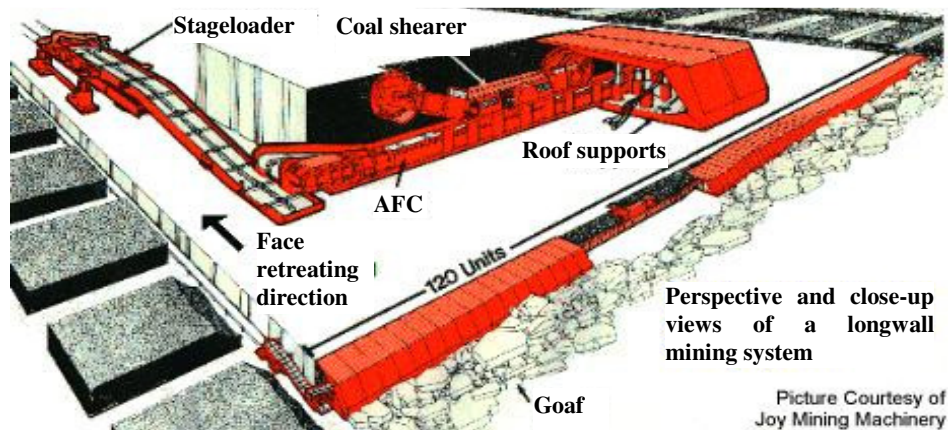


**Figure 1:** Schematic of a longwall mining system.

The longwall shearer is usually controlled by three operators who move along with it as it traverses the face. Its function is to rip the coal and push it into the AFC. In order to effectively accomplish these two tasks, the shearer is provided with two cutting drums. The stageloader is a machine that transfers the coal from the AFC onto the rubber belt conveyor. It is equipped with a flight conveyor chain that moves the coal from the input end towards the output or discharge end. Between the input and output ends, a crusher reduces large pieces of coal into smaller pieces that will not damage the rubber belt conveyor, and a sloped height rise known as the “goose

neck” raises the height of the transported coal from the AFC level to the rubber belt conveyor level.

### 3. EXPERIMENTAL SETUP

Due to spatial limitations encountered at underground coal mines, and, most importantly, due to the restrictions on electronic instrumentation that can create a risk of igniting methane in the atmosphere, the present study was conducted on a new stageloader at a Caterpillar assembly building. Figure 2 shows a panoramic view of the stageloader used for the test with its four main sections: The input end, the crusher, the goose neck, and the output end.

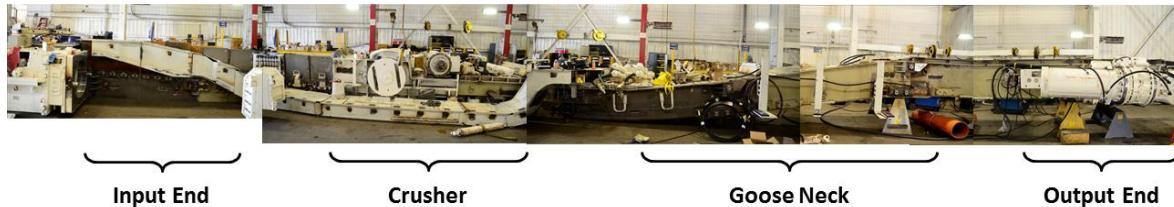


**Figure 2.** Panoramic view of the stageloader used for the test showing the four main sections: Input end, crusher, goose neck, and output end.

The room where the stage loader measurements were conducted is quite large –in contrast to the confined environment found in underground coal mines– with other activities being performed on the opposite end of the room such as forklift operations and welding. Specific room size measurements were not recorded. However, the following dimensions are given as approximations to give the reader a sense of scale. The length of the room is about 150 meters long and 25 meters across. The height of the room is about 15 meters. The floor near the stageloader was steel (about 0.02 meter thick) on top of concrete.

An AVEC, 1.5-meter-diameter array provided with 63 microphones was used for the test. Data were collected with the array at five different positions along one side of the stageloader as shown schematically in Figure 3. These positions were chosen in order to give a complete picture of the noise characteristics of the machine. The distance  $d$  shown in Figure 3 between the array plane and the stageloader side wall was 4.7 meters, and the center of the array was located at 1.6 meters from the floor.

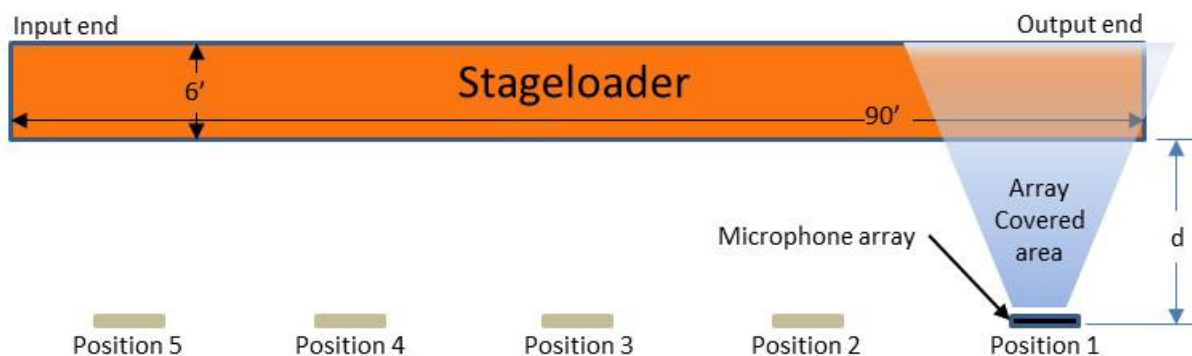


**Figure 3:** Schematic top view of the microphone array positions diagrammed relative to the stageloader.

For the present test, the conveyor chain was run empty, i.e. without coal, unlike normal operating conditions at underground mines where the stageloader is continuously transporting coal. In terms of testing time, it took approximately 2.5 hours to complete the entire test.

Data were collected simultaneously and continuously for all the channels at a sampling frequency of 51,200 Hz. A total of 32 seconds of data were collected for each record, providing sufficient data for 200 averages of 8,192 samples. Using these settings, the minimum frequency resolution was 6.25 Hz.

A calibration and picture alignment test was first performed with a speaker as the noise source. From this test it was determined that, in terms of spatial resolution, the phased array results were accurate at and above 500 Hz. Therefore, beamforming results were computed from 500 Hz to 20,000 Hz. However, since most of the sound radiated by the stageloader has low frequency content, i.e. less than 8,000 Hz, the acoustic maps and integrated spectra are reported only up to 8,000 Hz. Furthermore, since the present test is concerned with the determination of the spatial location and frequency content of the noise sources, the acoustic maps and array-integrated spectra presented in this paper are not A-weighted, i.e., unweighted.

#### 4. RESULTS

The main objective of the phased array measurements was to identify the noise sources on a stageloader and assess their frequency content. To this end, the acoustic maps were obtained with a conventional frequency domain beamforming algorithm, and then used to compute a spectrum for each array position. The most frequently used procedure to determine the spectrum levels from phased array measurements is the integration of the beamforming maps. Thus, for every frequency, the beamforming output over a region is added to obtain a single value. The integrated level,  $I$  is then obtained as:

$$I(V, f) = \int_V b(f, \vec{x}) d\vec{x} \quad (1)$$

where:  $V$  is an integration volume or area enclosing the noise source being quantified, and  $b(f, \vec{x})$  is the beamforming output at point  $\vec{x}$  for frequency  $f$ . However, note that with this approach the contribution from the sidelobes from the source being quantified are being added, and eventually, the sidelobes from other noise sources in the scanning field are also added. Notice also that changing the integration volume changes the integral output as a consequence of adding a different number of points. To account for these problems, two corrections proposed in the literature are used in this work<sup>5</sup>. The first correction attempts to eliminate the sidelobes from the integration and consists of integrating only the levels of the region  $V$  which values are within a given threshold from the peak level of the region. Usually this quantity is closely related to the array theoretical signal-to-noise ratio (the relative level between the mainlobe and the worst sidelobe). The second correction accounts for the number of points being integrated and the array response by using a normalization factor. This factor relates the integration output to the one obtained from beamforming a single source at the center of the scanning. These steps are taken to obtain the actual levels of the sources as would be measured by a single microphone at the center of the array.

Since there are a discrete number of points in the domain of integration, the normalized integrated spectra at frequency  $f$  can be written as:

$$I_{norm}(V, f) = \frac{\sum_n b_n(f)}{\zeta(f)}, \quad b_n > b_{max} - \delta \quad (2)$$

where:  $b_{max}$  is the maximum value in the beamforming map,  
 $\delta$  is a threshold set by the user, related to the array signal-to-noise ratio, and  
 $\zeta$  is the normalization factor given by:

$$\zeta(f) = \int_V p_0(\vec{x}, \vec{x}_0) d\vec{x}, \quad p_0 > p_{max} - \delta \quad (3)$$

where:  $\vec{x}_0$  are the coordinates of the center of the integration volume  $V$ , and  
 $p_0(\vec{x}, \vec{x}_0) = |\vec{w}^+(\vec{x})\vec{c}(\vec{x}_0)|^2$  is the array point spread function (*psf*) for a source at  $\vec{x}_0$ .

A comparison between the average microphone spectrum and the array-integrated spectrum at position 1 is shown in Figure 4. The array-integrated spectrum represents the noise at the center of the array produced by all noise sources in that region. The cutoff for the integration was set to 5 dB from the peak level in the integrated region. The difference in levels between the spectra in this plot is an indicator of the presence of additional noise (other sources in the machine or plant) that was eliminated through the beamforming process. For example, the levels of the average microphone spectrum near 1,000 Hz were about 5 dB higher than the array-integrated spectrum. For the low-frequency region from 560 Hz to 750 Hz, the difference between the two spectra is small—i.e. less than 3 dB. Comparison of these spectra indicates a significant amount of contaminating noise in the plant and from other regions of the machine. Note that the beamforming and integration process was only performed for frequencies above 500 Hz; thus no information is shown in the integrated spectrum below this frequency.

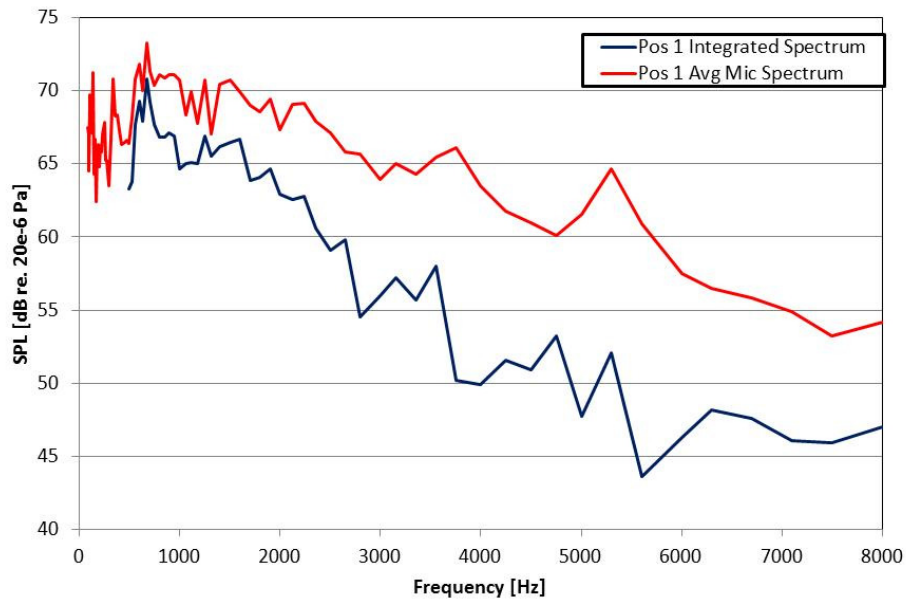


**Figure 4:** Comparison of average microphone spectrum and array-integrated spectrum at position 1 – 1/12<sup>th</sup> octave bands.

The integrated spectra for the five array positions are shown in Figure 5. This figure shows that the spectra for positions 1 and 2 have similar shapes. Position 1 was found to be the loudest while position 3 was the quietest. At frequencies below 800 Hz, Positions 1 and 2 have slightly higher noise levels than the other positions.

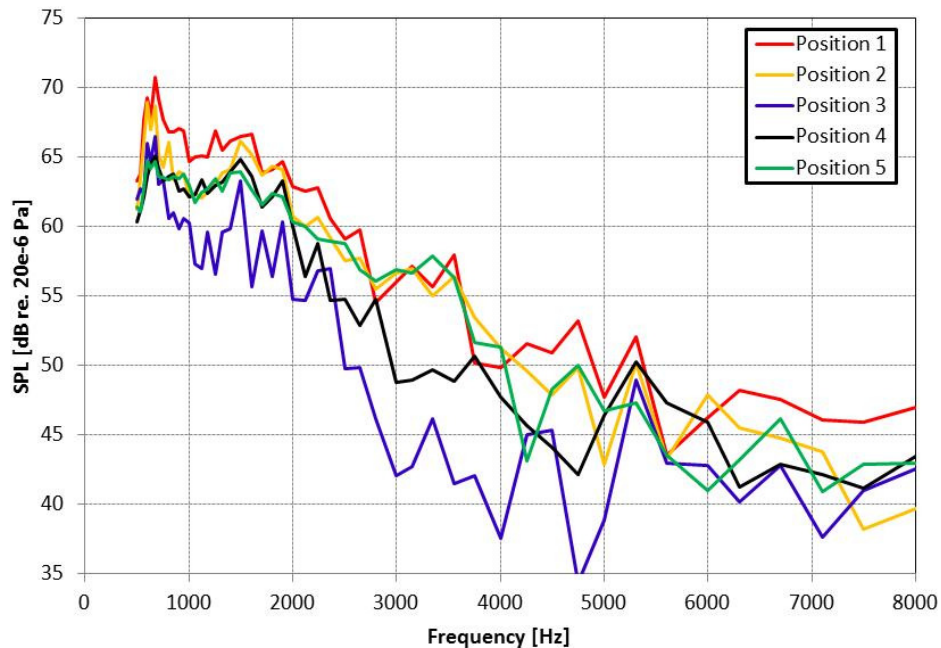


**Figure 5:** Comparison of the integrated spectrums for each of the five positions –  $1/12^{\text{th}}$  octave bands.

For brevity purposes, only the set of beamforming plots, i.e. acoustic maps, for the measurements at position 1 –found to have the highest sound levels– is presented in Figure 6. These maps correspond to the peaks on the integrated spectrum for this position shown in Figure 5. When observing these maps, note that they have different color scales. All beamforming maps are shown at the  $Z=0$  plane which is the location of the main side wall closest to the microphone array. The plots in these figures indicate that there are multiple noise sources on and around the stageloader. For the first frequency shown at 670 Hz (Figure 6a), there is a noise source coming from below the stageloader near the floor. It is suspected that this is a noise source from the stageloader reflecting off the floor. At 900 Hz (Figure 6b) and 1,250 Hz (Figure 6c) there are two noise sources on the lower part of the stageloader reflecting off the floor. At 1,600 Hz (Figure 6d) and at 1,900 Hz (Figure 6e), a noise source is seen near the end of the electric motor and around the collection of hoses on the main side wall (center of map). The next frequency shown at 2,240 Hz (Figure 6f) shows a noise source at the side wall of the stageloader. At 2,500 Hz (Figure 6g) and 3,550 Hz (Figure 6h) a noise source is seen near the end of the electric motor. Finally, at 4,750 Hz (Figure 6i) and 6,300 Hz (Figure 6j), there are noise sources at the side wall and at the top of the stageloader. It is suspected that impacts from the conveyor chain excite the return deck plates at the bottom, as well as the side wall plates on this enclosed section of the stageloader.

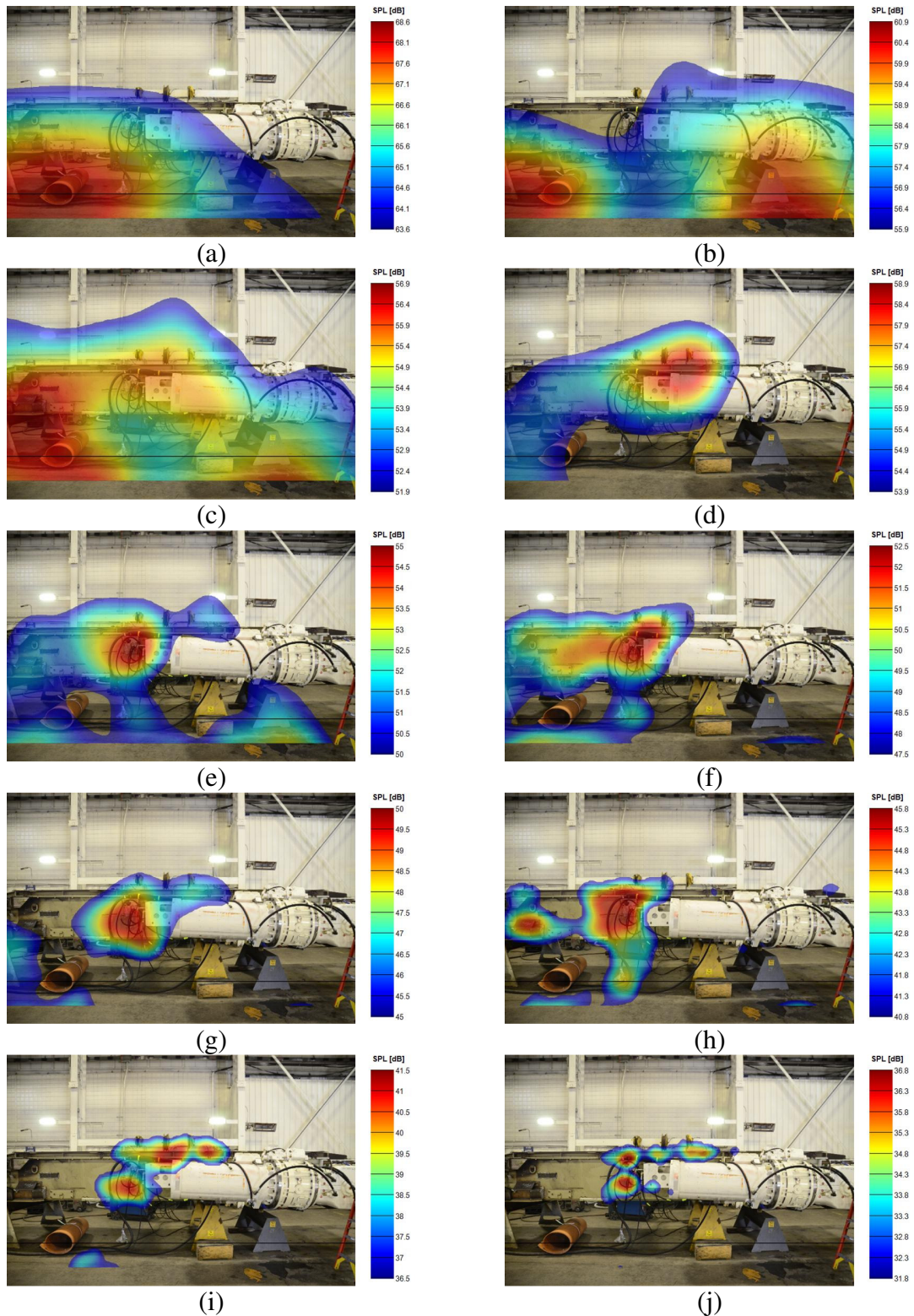


**Figure 6:** Beamforming maps for Position 1 at the  $Z=0$  location (plane of main side wall) for the following  $1/12^{\text{th}}$  octave bands: a) 670 Hz, b) 900 Hz, c) 1250 Hz, d) 1,600 Hz, e) 1900 Hz, f) 2,240 Hz, g) 2,500 Hz, h) 3,550 Hz, i) 4,750 Hz, and j) 6,300 Hz.

A more thorough investigation of the noise source locations at position 1 was performed by subdividing the integration region into three areas: left, middle, and right. These regions are shown in Figure 7. The integrated spectra for each of these regions are shown in Figure 8. The plot shows more noise is coming from the middle section at frequencies above 1,000 Hz.

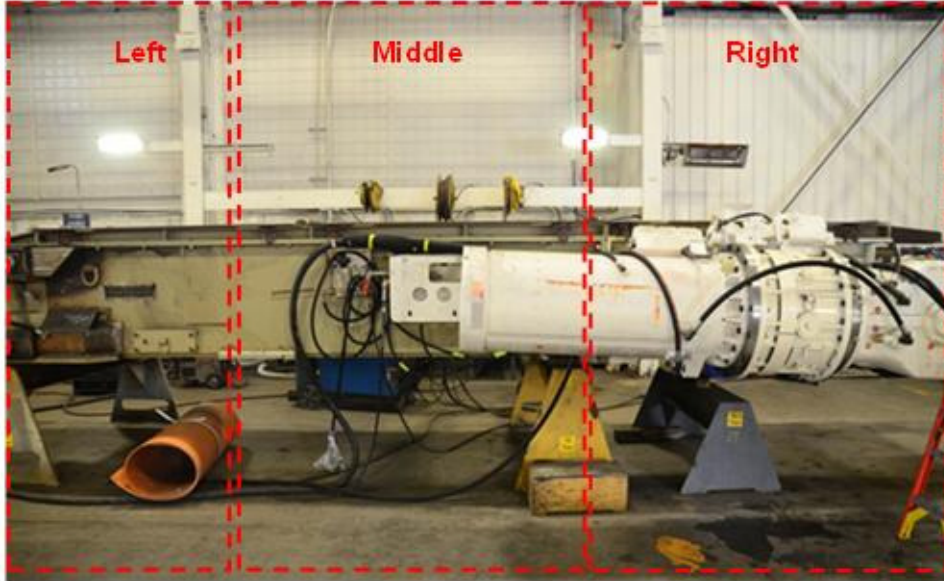


**Figure 7:** The integration regions at position 1, subdivided into “left, middle, and right” sections for a more detailed integrated spectrum analysis.

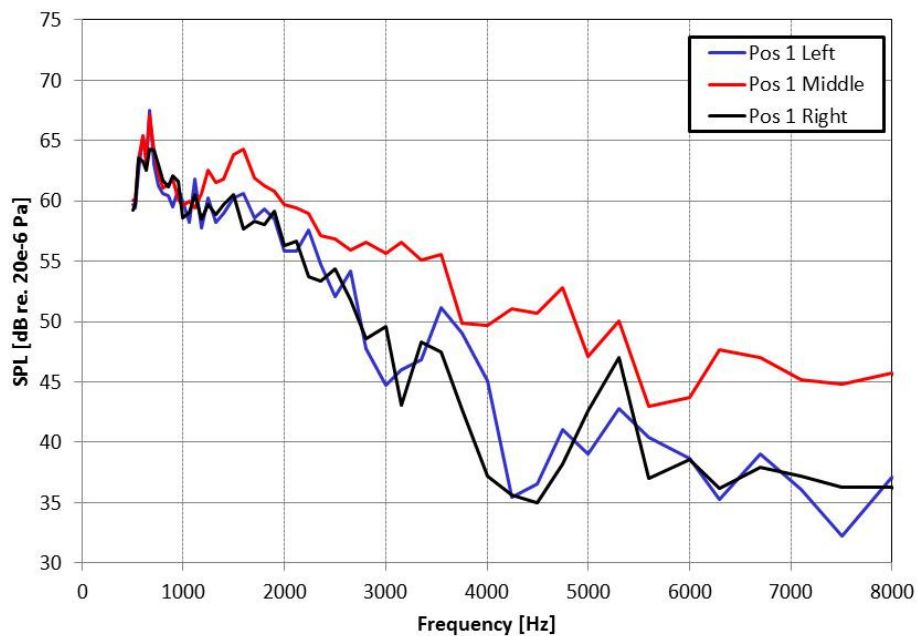


**Figure 8:** Integrated spectra for three different regions of integration with the array at position 1 – 1/12<sup>th</sup> octave bands.

## 5. CONCLUSIONS

Phased array measurements were performed on a stageloader machine at a Caterpillar assembly facility. Measurements were performed using a 63 microphone array in an open area plant

environment. Data were collected at five locations along the length of the stageloader. The main objective of the phased array measurements was to perform a preliminary identification of the noise sources on the stageloader and assess their frequency content. The results consisted of acoustic maps, array-integrated spectra, and average microphone spectra in the 1/12<sup>th</sup> octave bands. The most prominent noise sources tended to be at lower frequencies, i.e. below 1,900 Hz. The most dominant noise sources were in the region of the electric motor (Position 1) at the locations where the conveyor chain was either making noise itself or directly exciting other components such as the side wall plates or the conveyor return deck plates on the output side. It should be noted that the noise from the conveyor chain would be likely to change once coal is being transported. The presence of coal on the conveyor pan would add damping to these plates, and thus reduce the sound radiation. On the other hand, the acoustic levels may be higher when the stageloader is in a confined environment such as a coal mine.

These initial measurements provide the first insight on the location of the main noise sources and the actual noise levels generated across the spectrum on a stageloader. For noise control purposes, additional measurements (both acoustic and vibration) and analysis are needed to uncover the generation mechanisms and to design effective solutions.

### **ACKNOWLEDGEMENT**

The authors would like to thank CAT/Bucyrus for granting access to the stageloader and for all of its help during the actual test.

### **REFERENCES**

1. Spencer E.R., Babich, D.R., Alcorn, L.A., and Smith, A.K., Identification of Noise Sources on Longwall Panels Using Multiple Time-Synchronized Dosimeters, Transactions of the Society for Mining, Metallurgy, and Exploration, Vol. 322, 2007.
2. Title 30 of the Code of Federal Regulations CFR.
3. Pettitt Mark, R., and Slone, Robert, M., Noise Study of Longwall Mining Systems, Wyle Laboratories, Contract Report JO188072, 1986.
4. Longwall Census Table, Coal Magazine, February 2013.
5. Mueller, Thomas J. (Ed.), *Aeroacoustic Measurements*, Springer-Verlag, 2002.